Technical University of Denmark

Thermoeconomic Analysis Of a Gasification Plant Fed By Woodchips And Integrated With SOFC And STIG Cycles

Mazzucco, Andrea; Rokni, Masoud

Published in:
Proceedings of the 8th Conference on Sustainable Development of Energy, Water and Environment Systems

Publication date:
2013

THERMOECONOMIC ANALYSIS OF A GASIFICATION PLANT FED BY WOODCHIPS AND INTEGRATED WITH SOFC AND STIG CYCLES

Mazzucco Andrea
Department of Mechanical Engineering
Technical University of Denmark, Lyngby, Denmark
e–mail: andmaz@mek.dtu.dk

Rokni Masoud
Department of Mechanical Engineering
Technical University of Denmark, Lyngby, Denmark
e–mail: mr@mek.dtu.dk

ABSTRACT

This paper presents a thermo-economic analysis of an integrated biogas-fueled solid oxide fuel cell (SOFC) system for electric power generation. Basic plant layout consists of a gasification plant (GP), an SOFC and a retrofitted gas turbine with steam injection (STIG). Different system configurations and simulations are presented and investigated. A parallel analysis for simpler power plants, combining *GP*, *SOFC*, and hybrid gas turbine (GT) is carried out to obtain a reference point for thermodynamic results. Thermodynamic analysis shows energetic and exergetic efficiencies for optimized plant above 53% and 43% respectively which are significantly greater than conventional 10 MWe plants fed by biomass. Thermo-economic analysis provides an average cost of electricity for best performing layouts close to 6.4 and 9.4 c€/kWe which is competitive within the market. A sensitivity analysis of the influence of SOFC stack cost on the generation cost is also presented. In order to discuss the investment cost, an economic analysis has been carried out by involving main parameters such as Net Present Value (NPV), Internal Rate of Return (IRR), Time of Return of Investment (TIR) are calculated and discussed.

Keywords: gasification, wood chips, SOFC, STIG, techno-economic analysis, thermo-economic analysis.

INTRODUCTION

Primary aim of present study is to investigate innovative power plant solutions that might allow the use of a renewable source in a sustainable way, with greater thermodynamic performance and economic competitiveness than conventional technologies. In order to achieve such an objective, at first the renewable source, then a reasonable plant configuration have been selected. Cultivated biomass has been chosen due to the easiness of stocking this source in the form of wood chips. It follows that unlike other renewable sources, a continuous fuel feeding to the plant and in turn a continuous energy production can be guaranteed. To be more precise, poplar trees (*populus* genus) have been considered because of their composition features and the facility of having them growing in the Northern Hemisphere [1].

Sustainable exploitation is linked to cultivation area management. Subdividing it in four parts (one for seeding, two for growing and the last as the cutting zone) allows reaching a constant balance among cut trees and the grown ones. Such a system allows improvement environmental sustainability. A general overview of conventional power plants fed by biomass shows low values for both electrical efficiency and electrical power in comparison with standard fossil fuels plants such as Rankine cycle plants having a net electric power of about 10-20 MW with an efficiency of about 25-28 %; or even lower values when ORC (Organic Rankine Cycle) or Stirling engines are used. The main reason is that LHV (Lower Heating Value) of biogas is considerably lower than the LHV for natural gas (up to five times). Therefore, lower specific works will be obtained and consequently the electrical power could not be high enough when reasonable cultivation areas are considered. It follows that innovative plant technologies must be studied.

In this work an upscale of the Viking gasification plant has been considered [2]. Ahrenfeldt et al. [3] report that the Viking gasifier offers some interesting features such as low tar content in produced syngas (<5 mg/Nm^3), stable unmanned operation, high cold gas efficiency (>95%), low environmental impact (clean condensate, high carbon conversion ratio) and gasification process at ambient pressure. Since produced steam from the dryer is used as the heat carrier for the pyrolysis process, the two-stage gasification process is applicable for high moisture content fuels. This makes woodchips ideal for this process. Steam, as a gasification agent, is used to lower the operating temperature and increase process rate and the hydrogen (H2) content. The syngas produced in such gasifier is suitable to feed a SOFC, see Table 1.

Table 1. Syngas composition. Molar fraction.

Compound	Concentration
hydrogen	25.32 %
nitrogen	28.77 %
carbon monoxide	17.18 %
carbon dioxide	11.59 %
water (steam)	15.78 %
hydrogen sulfide	0.0045 %
methane	1.01 %
argon	0.35 %

Among different fuel cells under development today, an SOFC has been chosen because of its high operating temperature (ca. 700°C–1000°C) which allows the use of non-novel catalysts that are less expensive and insensitive to certain fuel contaminants [4 – 8] still present in the syngas. Furthermore also CO can be used as a fuel in an SOFC. In order to avoid catalyst poisoning, hydrogen sulfide is filtered in a gas cleaner. SOFCs are suitable of integration with gas turbine (GT) cycles [9, 10]. This enables to improve overall efficiency with respect to an individual system. However, the power ratio of SOFC to GT is high because SOFC is more efficient than GT in terms of energy conversion and total system cost when they are combined. Therefore, an improvement of GT efficiency is essential from such viewpoint. This can be achieved by using a high efficient gas cycle namely steam injected gas turbine (STIG) cycle.

A plant like IGSST (Integrated Gasification SOFC STIG) in which high efficiency commercially new technologies (GP and SOFC) and innovative solutions are integrated with well-known technologies (STIG) might bring additional ideas for using renewable sources in larger potentials to produce energy not only as sustainable but also as continuous energy source.

METHODOLOGY

After having estimated an initial value for overall plant efficiency and the mass flow rate of wood chips, a reasonable value for the cultivation area has been calculated striking a balance between the rise of power production and the increase of size of the cultivated area.
Initial values of interest have been calculated as P_{el}= 10 MWe and A_c= 47,6 km^2 (referring to an expected efficiency of 62%). In order to optimize the integration of the three sections (GP, SOFC and STIG), three different layouts have been proposed, differing in STIG solutions. Main results from thermodynamic analysis have been compared for each layout in order to identify the three best performing power plants.

Thermodynamic and thermo-economic analysis has been carried out using two different simulation tools. Since it is of interest here to investigate the systems in a stable design configuration, both analyses refer to a steady state approach.

IGSST CONFIGURATIONS

For each IGSST layout two cases have been considered: one with supplementary firing (TIT is set to 1180°C– *case A*) and one without supplementary firing (TIT follows the STIG upstream operating condition – *case B*). Figure 1 through Fig. 3 show the three different layouts without supplementary firing. When supplementary firing is needed, then the plant is modified by including a fuel splitter after the syngas blower so that fresh fuel can be injected into the catalytic burner. In all layouts syngas blower pressure ratio is limited to SOFC inlet temperature (650°C). For the bottoming cycle, three STIG cycle solutions can be distinguished, while topping cycles remain the same.

- Layout 1: After combustion, burned gases and steam are expanded in a STIG turbine and then sent to a HRSG, see Fig. 1. Heat from the exhaust gases is recovered to produce steam for injection (externally supplied demi-water). Since no steam turbine is used before injection and no particular temperature conditions are requested, the superheater (SH) is omitted in the HRSG in order to decrease the overall cost.

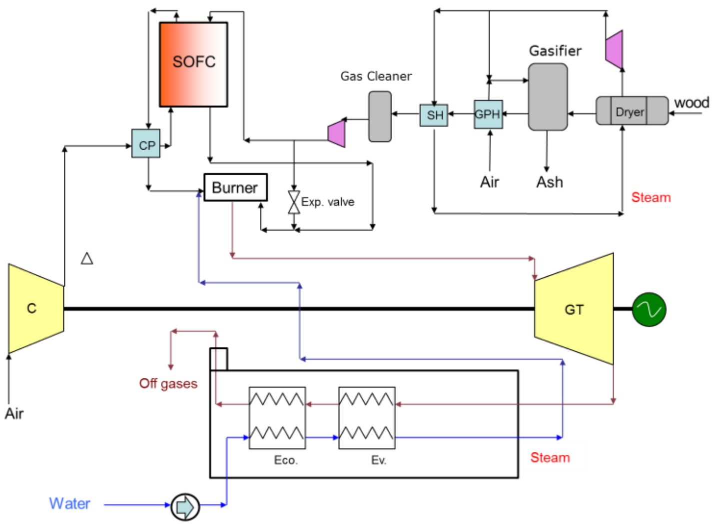

Figure 1. IGSST: Layout 1 with and without supplementary firing.

- Layout 2: A steam turbine is inserted right before the injection to recover the energy of the steam coming out of the HRSG, see Fig. 2. This is possible by including a SH in the

HRSG and producing high quality steam with suitable vapor quality, temperature (500°C) and pressure (40 bar). Mass flow rate of expanded steam is limited by injection purposes. Its ratio to the total exhaust gases´ mass flow rate is $r_{water-max}$= 15%.

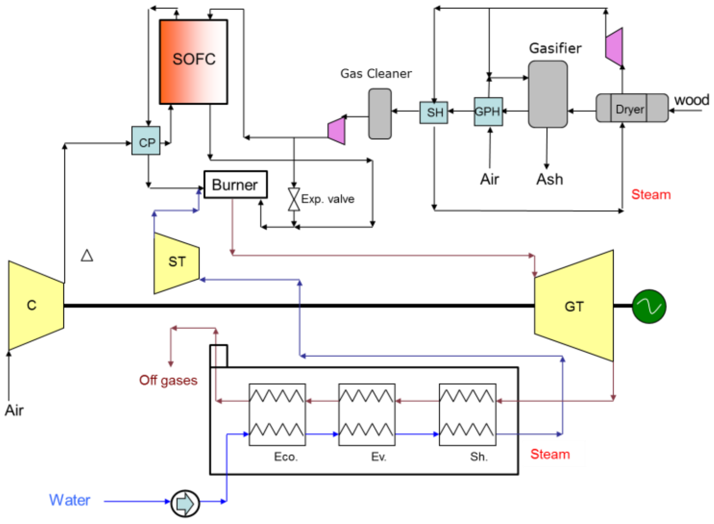

Figure 2. IGSST: Layout 2 with and without supplementary firing.

- Layout 3: A condenser is introduced in layout 2 in order to enable to recycle water in a closed loop, see Fig. 3. The large amount of cost associated with de-mineralized water in standard STIG cycles is then avoided. Thanks to water recycling, steam mass flow rate in the HRSG can be increased. Indeed the steam needed for injection is partially expanded and then drawn (respecting r_{water} limitation) while surplus steam is completely expanded in the ST. This enables to maximize total power by additional energy recovery at the ST.

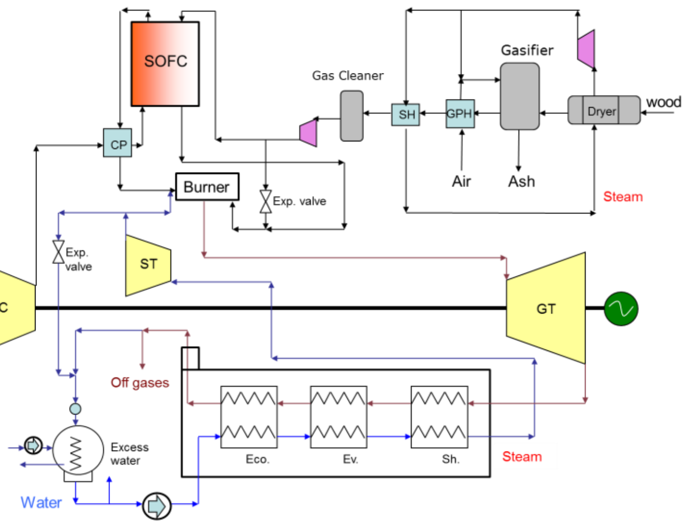

Figure 3. IGSST: Layout 3 with and without supplementary firing.

Reference power plants

In order to have a correct comprehension of the results, comparisons with similar and simpler plants have been carried out. Eight plant layouts have been studied which are related to four power plant typologies. Selected power plants for the comparison are basic ones; dual integrated plants (GP with SOFC, GT or STIG) are compared with respective triple integrated plants (GP-SOFC-STIG). They are all built up starting from the gasification section shown in Fig. 1 through Fig. 5.

Another configuration under study is an integrated gasification with SOFC and recuperated gas turbine as shown in Fig. 4. With and without supplementary firing are included by denoting expansion valve shown in the figure. Woodchips are dried and gasified first in a two-stage gasification and then are fed to the anode side of the SOFC. The off-fuels after the SOFC anode includes unburned fuel which is then send to the burner of a gas turbine. The recuperated gas turbine recovers some energy form exhaust off-gases at the same time that operating pressure of the SOFC will decrease considerably.

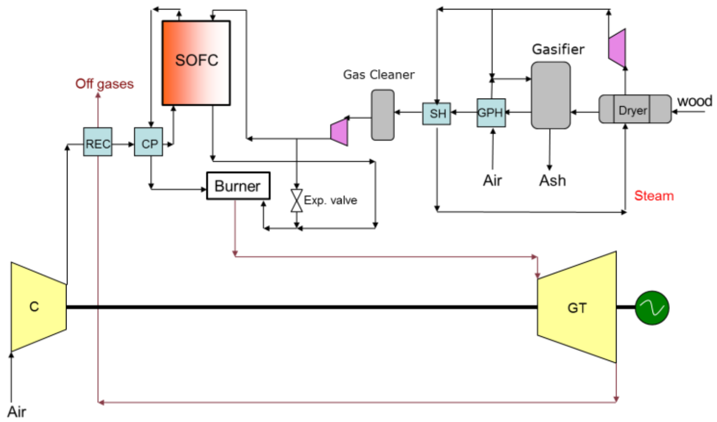

Figure 4. GP–SOFC–GT, Layout 2 includes a recuperator (with and without supplementary firing).

Table 2. Power plant typologies studied for comparison.

Dual section typologies	Triple section typologies
GP – SOFC (2 layouts)	GP – SOFC - GT (2 layouts)
GP – GT (1 layout)	
GP – STIG (3 layouts)	

Plants´ typologies are presented in Table 2 while the description of each plant is given below.
Dual section plants:

- GP – SOFC

  In this layout a gasification section followed by a SOFC unit with anode and cathode pre-heaters and a compressor to make the air circulate in the high pressure cathode circuit. Here, the anode pre-heater is needed to reach the SOFC inlet temperature of 650 °C, since the syngas temperature is not high enough for direct entering to the anode. The off-gases after the burner are dissipated directly to the environment.

  The second layout is represented in Fig. 5. Compared to the first layout two differences can be noticed. First of all a methanator section is introduced between GP and the SOFC in order to increase the CH_4 content in the syngas prior to the SOFC anode. It is composed of a methanator reformer and a reformer pre-heater (RP) to increase syngas temperature to the methanator operating temperature of 300°C. The reformed syngas composition is presented in Table 3 which can be compared to syngas composition shown in Table 1. As seen the methane content is increased by about 5 times on molar basis. Secondly, a recuperator is incorporated to recover heat from the combusted gases and preheat the air prior to the cathode pre-heater. As discussed in [4], these modifications are very effective for increasing the overall efficiency.

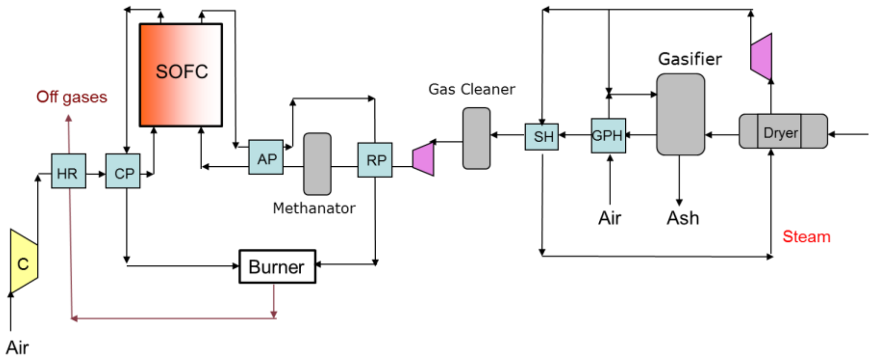

Figure 5. GP–SOFC, Layout 2 including Methanator and recuperator.

Table 3. Syngas composition after the methanator. Molar fraction.

Compound	Concentration
Hydrogen	22.09 %
nitrogen	31.22 %
carbon monoxide	8.80 %
carbon dioxide	18.31 %
water (steam)	14.64 %
methane	4.57 %
argon	0.37 %

- GP – GT
  In this layout, gasification plant is followed by a simple gas turbine. After syngas blower, the fuel is directly sent to the burner along with compressed air. Burned gases are expanded in the turbine and released to the environment without any heat recovery.
- GP – STIG
  Here, three layouts are studied which differs in the STIG solution after the gasification plant. These solutions are the same as explained in detail in the previous chapter and are shown in Figs. 1–3. No SOFC system is considered here and the syngas is compressed and then sent to the STIG section. Since fresh fuel is employed in the burner, it is possible to set the TIT to 1180 °C as for *case A* in the IGSST analysis.

Triple section plants:

- GP – SOFC – GT
  Two layouts are proposed and studied for such triple hybrid plants. One is obtained by replacing the STIG part in Fig. 1 with a gas turbine. No HRSG and steam injection are thus included, and the expanded exhaust gases are released to the environment without any heat recovery.
  In the second layout, as afore explained, it is suggested to include a recuperator after the gas turbine as shown in Fig. 4. Thus the difference between these two layouts is inclusion of recuperator to recover energy from the exhaust gases and preheat the air prior to the cathode preheater of SOFC. Compressed air is therefore preheated in two-steps before entering the SOFC cathode.

As for IGSST, also for GP–SOFC– GT plants *case A* and *case B* have been studied, with and without supplementary firing respectively.

THERMODYNAMIC AND EXERGY ANALYSIS

Thermodynamic and exergy analysis have been carried out by means of DNA (Dynamic Network Analysis) that is a component-based simulation tool for energy system analysis resulting of an ongoing development at the Department of Mechanical Engineering, Technical University of Denmark. DNA is a text-based application running through an editor window. Each component of the system is enclosed by a control volume and named. Components include a number of constitutive equations representing their physical properties, as well as relations for thermodynamic properties of the fluids involved.

Components´ branches are connected by numbered nodes in order to build the system. At the end 14 different DNA codes have been written, each of them refers to a particular plant solution. In order to optimize the results, different input values have been considered for each code such as number of stacks (NS) and U_f of SOFC. More than 50 simulations have thus been run. The solution is provided by solving a system of non-linear equations through the Newton Raphson modified algorithm [11]. The first two sections namely GP and SOFC have been maintained the same since the aim of the thermodynamic analysis is to evaluate plant performance improvement by recovering related wasted energy using different STIG cycle solutions. Input data are all devices features (i.e. compressors and turbines isentropic efficiencies have been set to 0.88 and 0.9 respectively), environmental state and mass flow values for inlet streams (mainly: air at the compressor, water at the HRSG and wood chips at the gasifier). The fuel mass flow and consequently other mass flows differ from each plant in order to deliver the desired power of 10 MWe. Main input data are reported in Table 4 while other input data which distinguish the performance of the corresponding layout are presented in Table 7, in the section for thermodynamic results.

Table 4. Main input data for all layouts.

Component	Parameter	Value	Unit
Dryer	T_{in} fuel side	15	°C
	p_{in} fuel side	1	bar
	T_{out} fuel side	150	°C
	T_{in} fuel side	150	°C
	p_{in} fuel side	1	bar
	Δp fuel side	0.005	bar
	Δp steam side	0.005	bar
	Heat loss	0	kW
Gasifier	T_{in} water	150	°C
	Operating p	0.998	bar
	OT	800	°C
	Δp syngas	0.005	bar
	Water-to-fuel ratio	0	–
	Carbon conversion factor	1	–
	Heat loss	0	kW
Air pre-heater	Δp syngas side	0.005	bar
	Δp air side	0.005	bar
	Heat loss	0	kW
Steam heater	T_{out} steam side	200	°C
	Δp syngas side	0.005	bar
	Δp steam side	0.005	bar
	Heat loss	0	kW
Steam blower	η_{is}	80	%

	η_m	98	%
Desulphurizer	Δp	0.0049	bar
	Heat loss	0	kW
Syngas blower	η_{is}	88	%
	η_m	98	%
	r_c	8.2	–
SOFC	T_{in} anode side	650	°C
	T_{in} cathode side	650	°C
	U_f	(0.7-0.85)	$kg_{used\text{-}fuel}/kg_{input\text{-}fuel}$
	OT	780	°C
	Δp anode side	0.01	bar
	Δp cathode side	0.005	bar
	Cells/stack	75	–
	Number of stacks	(4000-5000)	–
	Heat loss	0	kW
Cathode pre-heater	Δp flue gas side	0.008	bar
	Δp air side	0.008	bar
	Heat loss	0	kW
Burner	Heat loss	0	kW
Gas turbine	η_{is}	90	%
Electric generator	η_{el}	98	%
Air compressor	η_{is}	88	%
	η_m	98	%
	p_{in}	1	bar
	T_{in}	15	°C
Super heater	Δp steam gases	0.005	bar
	Δp exhaust gases	0.005	bar
Evaporator	Δp steam side	0.005	bar
	Δp exhaust gases	0.006	bar
Economizer	Δp water side	0.007	bar
	Δp exhaust gases	0.01	bar
Pump	η_{is}	95	%
Steam turbine	η_{is}	90	%

In order to allow comparisons among different sets of data, the environmental state for both thermodynamic and exergo-economic analysis refers to ISO conditions: T_0 = 15°C and p_0 = 1 bar. The analysis provides thermodynamic state and exergy values at each node together with energetic efficiency and electrical power production.

COST MODELING

The purpose of the cost modeling effort is to provide appropriate objective functions for optimal selection of system configuration and system design parameters. Lifespan, operating hours and other relative parameters are shown in Table 5.

Table 5. input data for cost rates assumed in the analysis.

Parameter	
Lifespan	20 years
Operating hours	7000 hr/yr
Interest rate	6 %
Rate of inflation	2 %
Construction period	1 years
Operating and maintenance factor	5 %
Currency conversion	1.31 €/$

Since thermoeconomic equations for most components (compressor, turbine, heat exchanger, etc.) are well-known [14], only equations for the gasifier and SOFC are described here in detail.

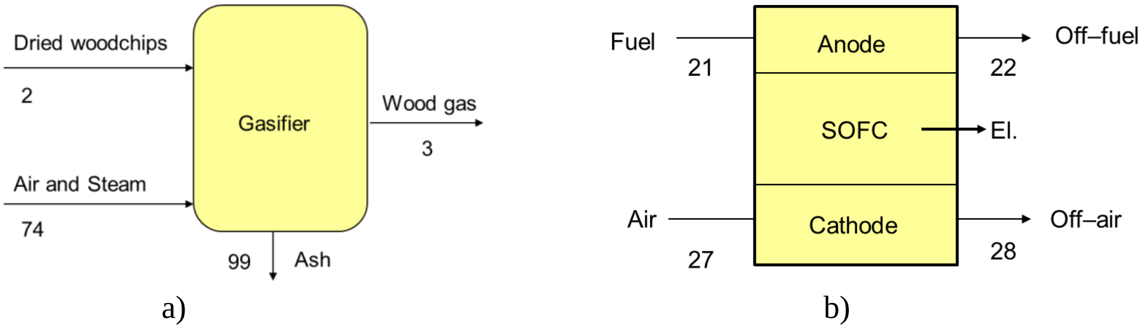

Figure 6. (a) gasifier, (b) SOFC model schemes

For the gasifier (referring to Fig. 6a), only the syngas is allocated as the product. The fuel is made up of steam-air mixture and dried woodchips. Cost and exergy balances are expressed by Eq. (1) to (5):

$$\dot{E}_{74} + \dot{E}_2 = \dot{E}_3 + \dot{E}_{99} + \dot{E}_{D,gasifier} \quad (1)$$

$$c_{74}\dot{E}_{74} + c_2\dot{E}_2 + \dot{Z}_{gasifier} = c_3\dot{E}_3 + c_{99}\dot{E}_{99} \quad (2)$$

$$\dot{E}_{L,gasifier} = \dot{E}_{99} \quad (3)$$

$$c_{99} = 0 \quad (4)$$

$$I_{gasifier} = 2{,}9 \cdot 10^6 \cdot (3{,}6 \cdot \dot{m}_{woodchips})^{0{,}7} \quad (5)$$

In order to make the system determined, the auxiliary Eq. (4) sets the cost of ash disposal in €/kWh equal to zero. Eq. (5) provides gasifier purchase cost ($) as a function of woodchips mass flow rate [12].

For the SOFC (as referred to Fig. 6b), exergy and cost balances are shown in Eq. (6) to Eq. (8) below

$$c_{21}\dot{E}_{21} - c_{22}\dot{E}_{22} + \dot{Z}_{SOFC} = c_{28}\dot{E}_{28} - c_{27}\dot{E}_{27} + P_{el} \quad (6)$$

$$\dot{E}_{21} - \dot{E}_{22} = \dot{E}_{28} - \dot{E}_{27} + P_{el} + \dot{E}_{D,SOFC} \quad (7)$$

$$\dot{E}_{L,SOFC} = 0 \quad (8)$$

A fuel cell integrated with a bottoming cycle can be described by different cost models, varying by *product* and *fuel* allocation [13, 14]. In this study the exergy difference between the outgoing used fuel and the inlet reformed gas is considered as *fuel*. Electric power and flue gas are considered as *product*. Thus auxiliary equations for SOFC will be

$$c_{21} = c_{22} \tag{9}$$

$$c_{P_{el}} = \frac{c_{28}\dot{E}_{28} - c_{27}\dot{E}_{27}}{\dot{E}_{28} - \dot{E}_{27}} \tag{10}$$

SOFC purchase cost in \$ (inverter cost is calculated separately) is derived from [15, 16] and adapted to present model. Eq. 11 provides a single SOFC's stack cost:

$$I_{stack} = 1800 \ \$/\mathrm{m}^2 \tag{11}$$

Expressing the unit cost of a single stack in [$/m^2$] instead of regularly used [\$/kW] is dictated by biogas characteristics. Due to fuel dilution from digester CO_2 content, a stack operates at a lower power density compared with a natural gas-fueled system. Therefore a larger active area is needed to ensure the required power output. The cost of an SOFC can vary with the production volume approximately between 150 – 1500 \$/kW. In this paper the cost of a fuel cell stack is determined based on a unit cost of 1620 $/m^2$ at a production volume of 100 MW/yr [16]. This value reflects the manufacturing cost of mature anode-supported planar cells with metallic interconnects. Since in the present study each stack has 75 cells with a cell active area of 144 cm^2, the unit cost does not account for a 10% discount related to scale-up to 500 cm^2 as suggested by Thijssen in ref. [16].

Regarding to the three different layouts, the stack number changes and so does the entire SOFC purchase cost. SOFC power output depends not only on the stack number but also on its operating condition (such as utilization factor, operating temperature, etc.) when operated within the plant configuration. Calculations show that the average value of SOFC purchase cost in this study is 1340 \$/kW. Maintenance cost for SOFC has been calculated following instructions in ref. [15] but since in our model each stack has a design power of 1.5 kW and a high number of stacks is required to obtain the total desired power, instead of 1 stack replacement every 5 years, here 8 stack replacements per year (12 kW) have been considered. This corresponds to a O&M factor of 4% as suggested in ref. [16] to stay on a safe side.

THERMO-ECONOMIC ANALYSIS

For each component "k" of the system operating at a steady state, the cost balance expresses that the cost rate associated with the "product" of the system ($\dot{C}_P$ [€/h]) equals the total rate of expenditures made to generate the product, namely the "fuel" cost rate ($\dot{C}_F$ [€/h]), and the cost rate associated with capital investment ($\dot{Z}^{CI}$ [€/h]) and operating and maintenance ($\dot{Z}^{OM}$ [€/h]), [17 – 19], as shown in Eq. (12). Analysis has been carried out with respect to TEC method.

$$\dot{C}_{P,k} = \dot{C}_{F,k} + \dot{Z}^{CL}_{TOT,k} + \dot{Z}^{OM}_{TOT,k} \tag{12}$$

At first, equations referring to PEC (Purchased Equipment Costs) have been implemented [20 - 24] and investment cost has been calculated for each component together with Direct Costs (DC) and Indirect Costs (IC), listed in Table 6. Capital investment I_k^{TOT} is amortized in *n* years as shown by Eq. (13):

$$\dot{I}_k^{TOT} = f \cdot I_k^{TOT} \tag{13}$$

Where *f* is the annuity factor defined by Eq. (14):

$$f = \left[\frac{q_i^{(n+CP)} - 1}{(q_i - 1) \cdot q_i^{(n+CP)}} - \frac{q_i^{CP} - 1}{(q_i - 1) \cdot q_i^{CP}} \right] \tag{14}$$

Where q_i is the interest factor defined by means of interest rate *int* and rate of inflation r_i as:

$$q_i = \left(1 + \frac{\text{int}}{100}\right) \cdot \left(1 + \frac{r_i}{100}\right) \tag{15}$$

Table 6. Economic values for cost rates assumed in the analysis.

TOTAL CAPITAL INVESTMENT (TCI)			
A. DIRECT COSTS (DC)		B. INDIRECT COSTS (IC)	
1. Onsite costs		i) Engineering + supervision:	8% PEC
a) Purchased – equipment costs (PEC)		j) Construction costs + C.Pr	15% PEC
b) Purchased – equipment installation	45% PEC	k) Contingency:	15% PEC
c) Piping:	35% PEC		
d) Instrumentation + controls:	20% PEC		
e) Electrical equipment + materials:	11% PEC		
2. Offsite costs			
f) Civil, structural + architectural work:	30% PEC		
g) Service facilities:	50% PEC		

Total investment cost (TIC) has been determined. From this, considering yearly operating hours of the plant, cost rates have been calculated and used to assemble cost balances.Exergy, cost balances and auxiliary equations have been assembled for each component to build up the linear system which has been solved by means of EES. Among them most important auxiliary equations are fuel and demineralized water costs: $c_{woodchips}$ = 85 €/ton [25], $c_{demi\text{-}water}$ = 0,000357 €/kg [26]. The analysis provides specific cost at each node together with evaluation parameters, Δr_k, f_k and electricity generation cost c_{el}.

THERMODYNAMIC RESULTS

Optimization has been carried out by running simulations with different values for main input parameters within reasonable range [27] by considering plant size, technical features, and economy-related aspects. In Table 7 input data for other components are shown. Only three best performing layouts are presented in the table refereeing as L1, L2, L3 (c.f. Table 9).

Table 7. Main input data for the optimized and best performing layouts.

Component	Parameter	L1	L2	L3	Unit
Dryer	m_{wood}	1.6	1.7	1.8	kg/s
SOFC	U_f	0.7	0.7	0.7	$kg_{used\text{-}fuel}/kg_{input\text{-}}$

					fuel
Burner	T_{out} combustion gases	free	Free	1180	°C
Super Heater	T_{out} steam p_{out} steam	–	–	500 50	°C bar
Air compressor	r_c	8.2	8.2	15	bar
Evaporator	p_{ev} steam	–	8.2	50	bar
Condenser	Δp water side Δp steam side T_{in} water side T_{out} water side Heat loss	–	–	0.01 0.01 15 35 0	bar bar °C °C °C
Recuperator	Pinch point	14	–	–	°C

By comparing the results obtained in Table 8 and 9, one may conclude that the triple hybrid plants perform best, which is due to major energy recovery in the system.

Table 8. Main results for reference power plants.

Plant type	Layout	Case	NS	P_n [MWe]	η [%]	ψ [%]
GP-SOFC	1	–	50000	9.63	33.78	29.37
	2	–	50000	9.57	33.58	29.19
GP-GT	1	–	–	9.4	28.93	25.25
GP-STIG	1	–	–	9.78	34.30	29.83
	2	–	–	9.57	40	34.75
	3	–	–	9.5	39	33.90
GP-SOFC-GT	1	A	4000	9.86	45.52	39.57
		B	6000	9.81	49.19	42.74
	2	A	5000	9.86	52.64	45.76
		B	4000	9.80	53.79	46.76

The GP-SOFC systems present slightly higher efficiency than the GP-GT ones: the SOFC is a higher efficient component (energy efficiency typically in the range of 45%-50% in a stand-alone case with reformed methane) than gas turbines. However it can be noticed that both systems do not reach their own standard efficiency values when are fueled by natural gas. Reasons are the energy absorption in the gasification plant as well as syngas composition.

For the triple hybrid plants (see Table 8 and 9) the increase in efficiency as it occurs between GP-GT and GP-STIG layouts, is not present which is due to limitations on fuel cell operating temperature and the fact that such plants are already relatively efficient. This in turn affects the bottoming gas cycle performance. Thus, the GP-SOFC-GT layout 2 - *case B* is selected as one of the three best performing plants and its performances are then reported below in Table 9 along with cultivation area estimation. Table 9 presents the best performing plants that show a good combination of high energy and exergy efficiencies and a power output close to 10 MWe.

Table 9. Main results for optimized best performing plants.

Plant type	Layout	Case	Name	Fig.	NS	P_n [MWe]	η [%]	ψ [%]	A_c [km^2]
GT-SOFC-GT	2	B	L1	4	4000	9.80	53.79	46.76	46.12
GP-SOFC-STIG	1	B	L2	1	5000	9.77	50.39	43.81	48.94
	3	A	L3	3	4000	9.95	48.48	42.22	51.78

For L1, power output is limited not only due to NS value but also due to the absence of steam injection. The efficiencies are high because of the optimized thermal coupling at the recuperator between turbine outlet gases (451°C) and the air stream heated from 274°C to 437°C (while gases are released to the environment at 315°C). L3 provides lower energy efficiency and slightly higher electric power (≥0.15 MWe) when compared to L2. Main reason for the relatively low efficiency is that in L3 the SOFC participates to total gross power output with only 3.19 MW and the biggest power production belongs to the bottoming cycle which is not as efficient as the fuel cell. Indeed for L1 and L2 SOFC power outputs are 6.05 and 6.92 MWe respectively. Regarding L3 power, this layout is TIT controlled (1180 ˚C, namely *case A*) while for L1 and L2 TIT are 857 ˚C and 689 ˚C respectively. It follows that for L3, burned gases are expanded with high efficiency in the gas turbine and on the other hand exhaust gases are much warmer than in L2 and L3. Therefore, produced steam is characterized by significantly better quality conditions (500°C and 50 bars for case A; 215,56 °C and 40 bars for case B, same layout) and higher energy is recovered at the steam turbine (0,82 MWe). Increasing NS or U_f in L3 results mainly in a small increase of efficiency while power output will almost be constant. This is due to the higher conversion of in the SOFC plant and consequently lower energy would be left for the bottoming cycle. This in turn results in a layout with nearly similar performance but with a higher SOFC PEC value.

Being power output nearly constant for all layouts, cultivation area A_c inversely follows the thermal efficiency.

THERMO-ECONOMIC RESULTS

In Table 10 calculated thermo-economic parameters for main components are listed. Eq. (16) defines such calculated factors (e.g. exergo-economic factor f_k and relative cost difference Δr_k).

Table 10. Relative cost difference and exergo-economic factor.

	L1		L2		L3	
Component	Δr_k [%]	f_k [%]	Δr_k [%]	f_k [%]	Δr_k [%]	f_k [%]
Gasifier	49.18	71.47	48.64	71.15	47.85	70.68
SOFC	25%	75.58	17.59	81.22	32.64	91.25
Recuperator / <u>HRSG</u>	81.69	4.55	<u>73.67</u>	<u>13.61</u>	<u>42.44</u>	<u>39.21</u>
Gas / <u>STIG turbine</u>	17.69	66.22	<u>19.82</u>	<u>73.27</u>	<u>13.05</u>	<u>70.8</u>

$$\Delta r_k = \frac{c_{P,k} - c_{F,k}}{c_{F,k}} \tag{16a}$$

$$f_k = \frac{\dot{Z}_k}{\dot{Z}_k + c_{F,k}\left(\dot{E}_{D,k} + \dot{E}_{L,k}\right)} \tag{16b}$$

Turbines show good values for both parameters. More precisely exergo-economic factor is within the optimum range of values for the component typology (35% < f < 75%).

Gasifier´s investment cost depends on biomass input; then decreasing plant size (instead of decreasing exergy efficiency) may allow obtaining a lower exergo-economic factor and therefore a more optimized system.

In addition, major attention should be given to those components where both exergy losses and total investment cost are high which are found to be recuperator for L1 and HRSG for L2, as shown in Table 10. Recuperator/HRSG's exergo-economic factor is very low for L1 and L2. In fact for these layouts the hot gases are released to the environment and inevitable high exergy losses then occur. Reducing temperature differences of heat exchangers would help to reduce exergy losses but in turn causes an increase of the investment cost. In this perspective an optimum value (lower than 55%) for heat exchanger´s exergo-economic factor can be obtained. Further, a future decrease in SOFC purchase cost or using a less efficient SOFC (higher exergetic losses) may provide a strongly reduce the f_{SOFC}'s value.

ECONOMIC ANALYSIS

Approach

In the investment analysis the process of achieving a desired objective involves resources and factors which are usually numerous and miscellaneous. The same outcome can be obtained by combining them in different proportions. In investment selection criteria one must always have a method available that allows comparing factors belonging to different natures. This issue is solved by allocating a cost proportional weight for each factor. Such factors can be classified as various information belonging to the technical, economical and temporal nature.

In the following it is assumed that objectives, bonds and outcomes can be completely monetized. Technical data are provided by thermodynamic analysis, while economic ones are partly given by exergo-economic analysis. Technical and economic information are then related to temporal dimension. In order to do so, it is usually needed a prevision analysis that includes the entire lifespan of investments.

Criteria for the selection of investment

Under former assumptions the ultimate aim of an investment is to achieve the maximum benefit. More precisely further analysis is placed within "classic" economics, in which desired benefit corresponds to net earnings. It follows that final decision will point to the solution for providing the maximum profit. Since environmental sustainability has been considered as a starting point, the economic analysis will allow choosing the most profitable system among environmentally friendly solutions. Economic methods for the selection of investment are usually divided in:

- Arithmetical methods: ROI (Rate of Investment), PB (Pay Back);
- Geometrical or financial methods: IRR, TIR, NPV and P_f (Profit factor).

Arithmetic methods do not take into account "time" as a monetary factor and therefore they can be generally applied to investment projects which either are distinguished by short lifespan or when short-time results are predominant due to future uncertainty. It follows that applying them to long time investment projects would provide unrealistic results.

Geometrical methods homogenize expenses and incomes by considering the instant at which they occur. Since for all systems a lifetime *n* of 20 years has been considered, in the following the analysis is carried out with financial methods. Eqs. (17) to (18) define internal rate of return *IRR* and profit factor P_f as in ref. [28].

$$IRR = a_{NPV=0} \qquad [\%] \tag{17}$$

where a is the discount rate that provides a NPV equal to zero.

$$P_f = \frac{NPV}{TIC}.100 \qquad [\%] \qquad (18)$$

Economic input data

From cost analysis gasifier has been found to be the most expensive component for all layouts, followed by the SOFC. A list of main input data, both calculated and assumed for the economic analysis is presented in Table 11. The appropriate discount rate here considered for calculations is the WACC (Weighted Average Cost of Capital) of the Company.

The electricity sell price for Denmark is obtained from ref. [29, 30] as a mean value for the year 2011.

Table 11. Economic input data values.

Quantity		L1	L2	L3
Total investment cost (TIC)	[M€]	65.43	72.25	71.43
Power plant lifetime	[years]	20 for all layouts		
Cost of electricity production	[c€/kWh]	6.54	6.38	9.35
Electricity selling price	[c€/kWh]	23.64 for all layouts		
Weighted Average Cost of Capital	[%]	8		

Results in Table 11 shows that the largest TIC value belongs to L2 which also has the lowest price for electricity generation. This might appear as a contradiction, but having the lowest cost of electricity generation does not inevitably result in the highest profitability. L2 and L3 have the highest fuel mass flows (1.7 and 1.8 kg/s respectively) which provide large gasifier investment cost as stated by Eq. (5). This also results in larger expenditures for the size of the entire system, as basically DC for piping and IC for engineering. Further, L2 has the highest NS resulting in the most expensive SOFC among all layouts. L2 and L1 present similar electricity generation costs, which is considerably lower than L3. Different are the reasons for that. Firstly, low generation cost for L1 is related to plant´s high thermal and exergetic efficiencies. Secondly, L2 has the major power output related to the SOFC which in turn results in a better allocation of its investment cost and therefore a reduced unit cost of *product* at the SOFC. It should be remembered that SOFC´s lowest relative cost difference among all layouts belongs to L2 which is due to its high power production. In Fig. 7 it is shown that the electricity cost layouts tends to be the same value, when SOFC PEC increases, and so being SOFC power output constant when the difference between L1 and L2 Δr_{SOFC} decreases. Same generation cost is reached for a stack price around 1900 €/m^2.

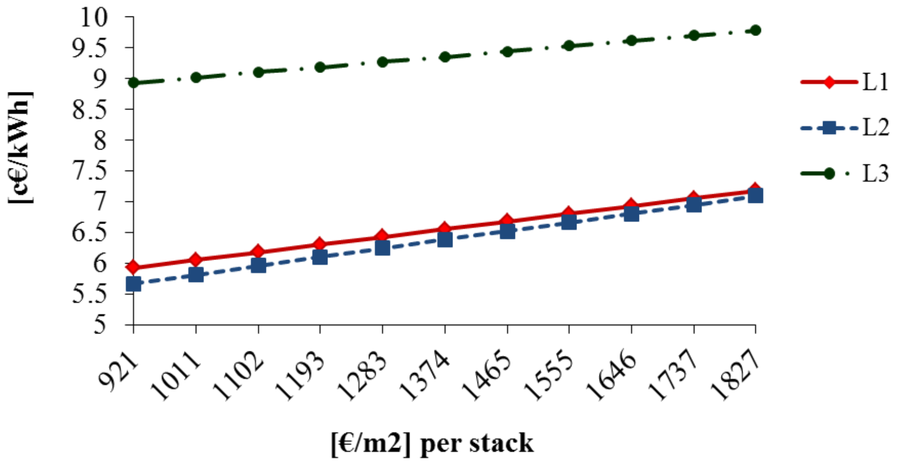

Figure 7.Cost of electricity generation as a function of stack cost.

Finally, unlike L2, L3 presents a high unit cost of *product* at the SOFC caused by a power output of only 3.19 MWe and resulting in the highest value of the relative cost difference. Furthermore this layout presents the highest fuel mass flow rate (1.8 kg/s) due to supplementary firing.

Cost modeling limitations

Due to extensive calculations a few simplified assumptions have been considered. All expenditures regarding the investment have been considered at the first year of construction and before the first year of plant´s operation. Sell price has been considered as a mean value and maintained constant for the entire lifespan of the plant, because it is impossible to accurately predict its future value for such a long period.

Since a large amount of water for the entire plant is needed (around 50.400 ton/yr for L2), it is not possible to buy it from a desalination company, though a demineralizing facility is needed. Considered water price refers to a fictitious purchase cost for the demineralizing facility. Similar considerations can be done for woodchips cost as it refers to a regular sell price for poplar woodchips in Europe.

Results of economic analysis

Calculated NPV for all layouts is listed in Table 12 while its year by year trend is given in Fig. 8a.

Table 12. Calculated economic parameters.

Quantity	L1	L2	L3
NPV [M€]	49.60	43.65	25.98
IRR [%]	17.2	15.5	12.5
P_f [%]	75.81	60.61	36.38
TIR [yr]	7.7	8.8	11

Net Present Value is positive for all layouts. Most profitable solution is L1. Indeed, despite that its generation cost is close to L2 cost of electricity, the L1 presents a much lower investment cost (see Table 11). The real time of the return of the investment is given by TIR which accounts for discounted cash flows and can be seen in Fig. 8a, when the time for which NPV has a zero value.

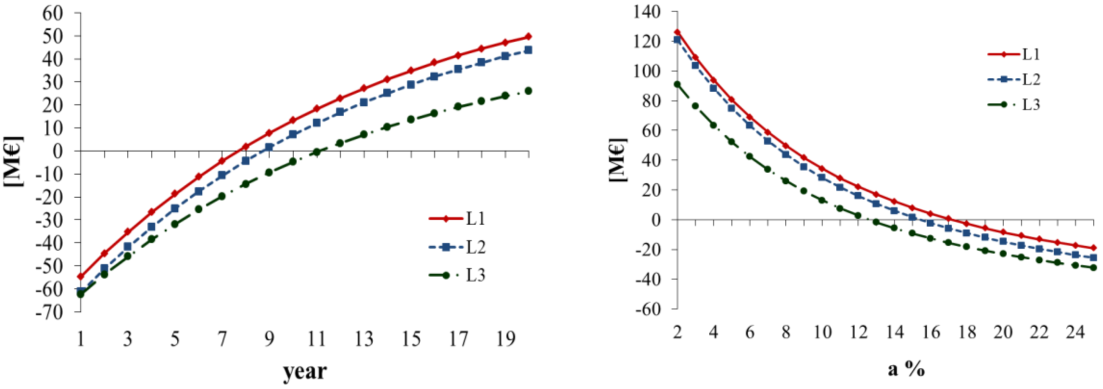

a) b)

Figure 8. (a) yearly NPV; (b) NPV as a function of discount rate.

Profit factor relates the net profit, accounting for the risk of investment to the total cost of the plant. As asserted in Eq. (18) it is calculated as a percentage of the ratio between NPV and TIC. The meaning of Fig. 8b is that each point of the curve represents the NPV after 20 years of the investment calculated at a discount rate *a*. Such curves are used to give a view of NPV dependency on the risk related to the investment and of the internal rate of return for each plant solution. It is easy to see that at a discount rate value of 8% NPVs correspond to the values listed in Table 12 and shown in Fig. 8a.

CONCLUSIONS

In this paper a techno-economic analysis of integrated power plants combining gasifier, SOFC and gas/STIG cycles is performed. Based on system modeling results and economic analysis the following conclusions are drawn:

- Gasification technology enables biomass use with high thermal efficiency when combined with an SOFC and a gas turbine as a bottoming cycle for a total power output of 10 MWe. This is true especially when the recovery cycle is composed by a gas turbine with a recuperator right before the cathode pre-heater of the fuel cell, due to a good temperature coupling. Optimized plants reach nearly 53.8% of thermal efficiency. The expected increase in efficiency when considering an advanced STIG cycle is not achieved since such a cycle requires high energy gases at the turbine and high temperature off gases to produce steam for injection. In this case then a better exploitation of STIG cycle leads to a lower use of the SOFC, which is the most efficient component. To reach the desired power output, supplementary firing is needed and so greater fuel mass flow rates which in turn bring an increase of the entire system´s energy input and a decrease of efficiency. Bigger plants with a power output higher than 10 MWe and with higher energies to be recovered and might solve this problem but they would be not feasible in terms of landfill extension.
  Finally the best option is to maintain SOFC power output fixed and having a gas turbine coupled with a recuperator that follows upstream conditions.
- Generation costs for electricity are provided by the thermo-economic analysis along with exergo-economic factors and relative cost differences for each component. Main sources of exergy inefficiencies are allocated at the recuperator for the layout with a simple gas turbine down-line of the SOFC section, and in the HRSG for the plant with the simplest open cycle STIG configuration, because gases with high energy are release to the environment instead of being recovered. For these layouts generation costs are found to be similar, as explained before, while for L3 the cost is around 45% higher. Low SOFC power output, high *TIC* and fuel mass flow rate seem to be reason for that. However electricity cost is lower than considered sell price for all solutions.

- With no incentives from governments it is unlikely that such plants can be actually built. Indeed having a positive *NPV* is not enough to ensure the convenience of the investment. Beside *NPV* value, also *TIR* must be considered along with the required threshold profitability from the investors. Expensive solutions with a long payback time (as power plants usually are) regularly require a P_f higher than 100% to be attractive from investors´ point of view. Same outcome is provided when considering *IRR*. Its calculated value has to be compared with the minimum acceptable rate of return required from the investors. Even though no rule can univocally be found it is easy to understand that in reality big initial expenditures need high discounted rates to account for the risk of the investment.

SOFCs offer an efficient way of utilizing biogas when combined with a gas turbine and recuperator for additional energy recovery in a 10 MWe system. Electricity generation costs successfully compete with costs of other power technologies if mature stack costs are realized. SOFC-based solutions integrated with an advanced STIG cycle might significantly increase the overall efficiency performance and offer further economic incentive to adopt the technology when providing a total power output above 10 MWe.

NOMENCLATURE

r_c	compressor ratio [-]
r_{water}	water ratio [%] or [$kg_{water}/kg_{exhaust}$]
η	energetic efficiency [-]
ψ	exergetic efficiency [-]
T	temperature [°C]
OT	operative temperature [°C]
TIT	turbine inlet temperature [°C]
p	absolute pressure [bar]
C.Pr	construction profit [%]
$\dot{Z}$	component cost rate [€/h]
U_f	utilization factor [-]
P	power [kW]
Hr	plants´ operating hours [hr/yr]
$\dot{C}$	cost rate [€/h]
$\dot{E}$	exergy flow [kW]
m	mass flow [kg/s]
n	equipment lifespan [years]
M	maintenance factor [-]
A_c	cultivation area [km^2]
CP	construction period [years]
L_{cell}	cell length [m]
Δr	cost difference factor [%]
f	exergo-economic factor [%]
a	discount rate [%]
n_{cell}	number of cell per stack [-]
η_{is}	isoentropic efficiency [%]
η_m	mechanical efficiency [%]
η_{el}	electric efficiency [%]
Δp	pressure drop [bar]

Abreviations

DC	Direct Cost
DNA	Dynamic Network Analysis
EES	Engineering Equations Solver
HHV	High Heat Value
HRSG	Heat Recovery Steam Generator
IC	Indirect Cost
IGSST	Integrated Gasification SOFC STIG
IRR	Internal Rate of Return
LHV	Low Heat Value
NPV	Net Present Value
NS	Number of Stacks
PB	Payback time
PEC	Purchase Equipment Cost
P_f	Profit factor
ROI	Return On Investment
SOFC	Solid Oxide Fuel Cell
TEC	Theory of the Exergetic Cost
WACC	Weighted Average Cost of Capital
TIR	Time of Return on Investment

Superscripts

0	reference state or ideal part
r	residual part
OM	operating and maintenance cost
TOT	total

Subscripts

e	electric
f	factor
k	k-th component
D	destroyed
F	fuel
L	lost
P	product

REFERENCES

1. D Cocco, C Palomba, P Puddu, Tecnologie delle energie rinnovabili, SGE Editoriali, Padova 2008.
2. JD Bentzen, MR Hummelshøj, U Henriksen, B Gøbel, J Ahrenfelt and B Elmegaard, Upscale of the two-stage gasification process, *Proc of 2 world conference and technology exhibition on biomass for energy and industry*. 10-14 May, Rome Italy, 2004; 1004-1007.
3. J Ahrenfeldt, U Henriksen, TK Jensen, B Gøbel, L Wiese, A Kather, et al Validation of of a continuous heat and power (CHP) operation of a two-stage biomass gasifier. J Energy Fuels 2006; 20:2672-80.
4. M Rokni, Thermodynamic Analysis of an Integrated Solid Oxide Fuel Cell Cycle with a Rankine Cycle, Energy Conversion and Management 2010; 51 (12):2724–2732.

5. J Larminie, A Dicks. Fuel Cell System Explained, John Wiley & Sons. ISBN: 978-0-470-84857-9
6. KM Keegan, M Khaleel, LA Chick, K Recknagle, SP Simner, J Diebler, Analysis of a planar solid oxide fuel cell based automotive auxiliary power unit, SAE Technical Paper Series No. 2002-01-0413; 2002.
7. Y Matsuzaki, I Yasuda. Electrochemical oxidation of H2 and CO in a H2-H2-COCO2 system at the interface of a Ni-YSZ cermet electrode and YSZ electrolyte, J Electrochemical Soc 2000; 147: 1630e5.
8. JW Kim, AV Virkar. The effect of anode thickness on the performance of anode e supported solid oxide fuel cell. *Proc. of the Sixth Int. Symp. on SOFCs* (SOFC e VI), PV99-19. J. Electrochemical Society 1999: 830-839.
9. RA Roberts, J Brouwer. Dynamic simulation of a pressurized 220 KW solid oxide fuel cell – gas turbine hybrid system: modeled performance compared to measured results. J Fuel Cell Science Technology 2006;3:18-25.
10. P Costamagna, L Magistri, AF Massardo. Design and part-load performance of a hybrid system based on a solid oxide fuel cell reactor and a micro gas turbine, J Power Sources 2001;96:352-368.
11. M Rokni, Plant characteristics of an integrated solid oxide fuel cell and a steam cycle. J Energy 2010;35:4691-4699.
12. D Gerhardt, J Blaney. Investment decisions for base load power plants, National Energy Technology Laboratory, ICF International; 2010: 402/012910.
13. A Arsalis, MR von Spakovsky, F Calise. Thermoeconomic Modeling and Parametric Study of Hybrid Solid Oxide Fuel Cell-Gas Turbine-Steam Turbine Power Plants Ranging From 1.5 MWe to 10 MWe. J. ASME Fuel Cell Technology 2009;6:011015-1.
14. A Bejan, G Tsatsaronis, M Moran. Thermal Design & Optimization, John Wiley & Sons Ltd, 1996.
15. AA Trendewicz., RJ Braun. Techno-economic analysis of solid oxide fuel cell-based combined heat and power systems for biogas utilization at wastewater treatment facilities. J Power Sources 2013;233:380-393.
16. JHJS Thijssen, The impact of scale-up and production volume on SOFC manufacturing cost, Technical report, Pittzburg, 2007.
17. A Marc, A Rosen, A concise review of exergy-based economic methods. EE'08 Proceedings; 3rd IASME/WSEAS international conference on Energy & Environment.
18. SB Ferreir, Thermo-economic analysis and optimization of biomass fuel gas turbines, *Phd thesis*, Cranfield University, Cranfield, 2002.
19. A. Toffolo, A. Lazzaretto. A new thermoeconomic method for the location of causes of malfunctions in energy systems. J Energy Resources Technology 2007;129:1-9, ISSN: 0195-0738, doi: 10.1115/1.242496040.
20. APER, Studio sui costi di produzione di energia elettrica da fonti rinnovabili.
21. MA Lozano, A Valero. Theory of exergetic costs, J Energy 1993;18:939-60.
22. AV Bridgwater. The technical and biomass gasification for power generation. J. Fuel 1995;74:631-53.
23. ZT Lian, KJ Chua, SK Chou, A thermoeconomic analysis of biomass energy for trigeneration. J Appl. Energy 2010;87:84-95.
24. JR Braun, Techno-Economic optimal design of solid oxide fuel cell systems for micro-combined heat and power applications in the U.S.. J Fuel Cell Science and Technology 2010;7(3): 031018
25. F Burger, W Sommer, Von der pappel bis zum Hackschnitzel, LWF, Berlin 2003.
26. E Curcio, E Drioli, F Macedonio, Integrated membrane systems for seawater desalination.

27. J L Silveira, CE Tuna, Thermo-economic analysis method for optimization of power systems – part II, Sao Paulo State University, Sao Paulo, 2002.
28. P Berra, L De Paoli, G Zingales, Economia delle fonti di energia, Cleup Editrice, Padova, 1997.
29. http://www.nordpoolspot.com.
30. Energy statistics 2011. Danish energy agency. 2011.